Asymmetrical-Flow Field-Flow Fractionation with On-Line Multiangle Light Scattering Detection. 1. Application to Wormlike Chain Analysis of Weakly Stiff Polymer Chains

ARTICLE *in* BIOMACROMOLECULES · MARCH 2003

Impact Factor: 5.75 · DOI: 10.1021/bm025706v · Source: PubMed

6 AUTHORS, INCLUDING:

Rheo Takahashi
Gunma University
40 PUBLICATIONS **611** CITATIONS
SEE PROFILE

Saphwan Al-Assaf
University of Chester
117 PUBLICATIONS **1,683** CITATIONS
SEE PROFILE

Kenji Kubota
Gunma University
156 PUBLICATIONS **4,496** CITATIONS
SEE PROFILE

Asymmetrical-Flow Field-Flow Fractionation with On-Line Multiangle Light Scattering Detection. 1. Application to Wormlike Chain Analysis of Weakly Stiff Polymer Chains

Rheo Takahashi,*,† Saphwan Al-Assaf,† Peter A. Williams,† Kenji Kubota,‡ Akio Okamoto,§ and Katsuyoshi Nishinari||

Centre for Water-Soluble Polymers, The North East Wales Institute, Plas Coch, Mold Road, Wrexham, LL11 2AW, U.K., Department of Biological and Chemical Engineering, Faculty of Engineering, Gunma University, Kiryu, Gunma 376-8515, Japan, Research Center, Denki Kagaku Kougyou Company, Ltd., Asahimachi, Machida, Tokyo 194-8560, Japan, Department of Food and Human Health Sciences, Graduate School of Human Life Science, Osaka City University, Sumiyoshi, Osaka 558-8585, Japan

Received October 22, 2002; Revised Manuscript Received December 7, 2002

Four samples of hyaluronan in the sodium form, ranging in weight-average molecular weight, M_w, from 6.67×10^5 to 4.23×10^6 were investigated by asymmetrical-flow field-flow fractionation coupled to multiangle light scattering (FlFFF−MALS) in 0.2 M aqueous NaCl at 25 °C. M_w and *z*-average radii of gyration, R_{Gz}, obtained via FlFFF−MALS showed a good agreement with the results obtained by conventional static light scattering. Furthermore, the molecular weight dependence of the radius of gyration for sodium hyaluronan obtained via FlFFF−MALS was analyzed on the basis of the Kratky−Porod model for unperturbed wormlike chains combined with the Yamakawa theory for radius expansion factor, and a sufficiently good agreement was observed between the theoretical prediction and experimental data. These results show the potential usage of FlFFF−MALS regarding size separation and molecular characterization even for weakly stiff chains.

Introduction

Understanding the dimensional properties of polymer chains has long been a major focus of the researches in polymer sciences, both theoretically and empirically. The overall conformations of polymer in solution have been estimated through comparing experimental data with theoretical prediction. Among the many models proposed for stiff polymer chains, the most typical one is the wormlike chain, or KP chain, which is a coarse-grained continuous chain having bending energy, introduced by Kratky and Porod.[1] Later, Yamakawa and his collaborators generalized the KP chain model by introducing torsional energy, and formulated various static and dynamic properties of helical wormlike chains including the KP chain as a special case.[2] This model expresses flexible random coils, regular helices, and rigid rods as limiting cases of its model and describes various possible intermediate structure of polymers. By using this model, the chain stiffness, chain diameter, monomer length, and the additional helical wormlike chain parameters in polymer solution can be determined.[3] The wormlike chain analysis, however, needs experimental data of steady transport coefficients or radii of gyration on highly monodisperse samples. In regard to polydisperse samples, appropriate statistical processing to compensate the polydispersity effects is required in the analysis. When persistence length, one of the wormlike chain parameter characterizing chain stiffness, is calculated by omitting such a statistical processing, it may be significant.[4] Therefore, using monodisperse samples is essential in wormlike chain analysis, or the correction of polydispersity effects is required for polydisperse samples. In the latter case, we need the determination of precise molecular weight distribution functions of the samples.[4,5]

Determination of molecular weight distribution is normally carried out by size exclusion chromatography (SEC) connected with a suitable detector. This method, however, has a few restrictions that prevent the analysis of some polymers. A problem often observed is that the polymer may adsorb, either completely or partly, to the porous gel in the columns. Another problem is the total exclusion of very high molecular weight molecules having large dimensional size from the pores of the packing material, and then the sample will not be fractionated. In addition, it has also been reported that degradation of high molecular weight polymers may occur[6] due to the high shear forces generated in the SEC columns during the elution. Flow field-flow fractionation[7] (FlFFF) is an alternative separation technique to separate molecules by size. It overcomes potential problems of shear degradation and adsorption onto the column packing. Furthermore, it is able to fractionate polymers of very high molecular weight. If FlFFF is coupled to multiangle light-scattering (MALS),

* To whom correspondence should be addressed. rheo_t@hotmail.com. Present address: Department of Food and Human Health Sciences, Graduate School of Human Life Science, Osaka City University, Sumiyoshi, Osaka 558-8585, Japan.

† The North East Wales Institute.

‡ Gunma University.

§ Denki Kagaku Kougyou Co., Ltd.

|| Osaka City University.

10.1021/bm025706v CCC: $25.00
Published on Web 01/22/2003

molecular weight distribution and the corresponding size distribution are estimated simultaneously.[8]

Hyaluronan is a typical weakly stiff chain. In 1995, Norisuye et al.[9] reported that sodium hyaluronan (NaHA) in 0.2 M NaCl is a stiff polysaccharide affected by the excluded-volume effects except for $M_w < 10^4$, and the intrinsic viscosities of nearly monodisperse samples are well described by the wormlike chain model. Excluded-volume effects were analyzed by using the Yamakawa theory[10−14] with Barrett[15] and Domb−Barrett[16] functions for the expansion factor. They obtained the wormlike chain parameter set of $q = 4.2$ nm, $M_L = 405$ nm^{-1}, $d = 1.0$ nm, and $B = 3.4$ nm. Subsequently, Tsutsumi and Norisuye[17] restudied the wormlike chain behavior of nearly monodisperse NaHA, and concluded that M_L values are almost constant (405 ± 5 nm^{-1}) in aqueous NaCl solution from 5 mM to 2.5 M, although B value in 0.2 M NaCl was revised to 4.0 nm. This value of $M_L = 405$ nm^{-1} corresponds to the disaccharide unit of 1.0 nm along the chain contour, and is quite reasonable according to the molecular structure. They also performed wormlike chain analysis of the dimensional properties, but in the course of the analysis, they corrected the effect of polydispersity for the measured radii of gyration R_{Gz} using a relation $R_{Gw}^2 = R_{Gz}^2 M_w/M_z$ with $M_w/M_z = 1.1$, where the subscripts w and z denote weight-averaged and z-averaged quantities, respectively. Thus, R_{Gz} data obtained from conventional static light scattering must be corrected even for nearly monodisperse samples in wormlike chain analysis.

Here we report the study of characterization of high molecular weight hyaluronan in 0.2 M NaCl using FlFFF−MALS. Applicability of FlFFF to size separation for weakly stiff chains was verified using high molecular weight samples. First, weight-average molecular weights and z-average radii of gyration obtained from FlFFF−MALS are compared with those obtained from conventional static light scattering. Finally, the molecular weight dependence of radius of gyration for hyaluronan was analyzed by perturbed wormlike chain model for dimensional properties.

Theory

Dimensional Properties of Perturbed Wormlike Chains. The well-known formulation for the mean-square radius of gyration of an unperturbed wormlike chain[18] is written as

$$R_{G,0}^2 = \frac{L}{6\lambda} - \frac{1}{4\lambda^2} + \frac{1}{4\lambda^3 L} - \frac{1}{8\lambda^4 L^2}[1 - \exp(-2\lambda L)] \quad (1)$$

where L is the contour length of the chain related to the molecular weight M by $L = M/M_L$, with M_L being the shift factor. In the limit of $\lambda L = 0$ and ∞, eq 1 gives the expressions for straight rods and Gaussian coils, respectively. For the perturbed wormlike chain, the radius of gyration is expressed as

$$R_G = \alpha_G R_{G,0} \quad (2)$$

where α_G is the expansion factor for the radius of gyration. This factor is a universal function of the scaled excluded-volume parameter $\tilde{z}$ and is known to be well reproduced by the Yamakawa theory[12−14] with the Domb−Barrett function.[16] The expression derived is

$$\alpha_G = [1 + 10\tilde{z} + (70\pi/9 + 10/3)\tilde{z}^2 + 8\pi^{3/2}\tilde{z}^3]^{2/15}[0.933 + 0.067\exp(-0.85\tilde{z} - 1.39\tilde{z})] \quad (3)$$

with

$$\tilde{z} = (3/4)(3/2\pi)^{3/2}\lambda B(\lambda L)^{1/2}K(\lambda L) \quad (4)$$

In this equation, $K(\lambda L)$ is a function of Kuhn's statistical segment number given by Shimada and Yamakawa,[14] and B is the excluded-volume strength standing for the interaction between a pair of beads. For the wormlike chain as a limit of the helical wormlike chain, we have $\lambda = 1/2q$ and $B = \beta/b^2$ with q, β, and b being the persistence length, binary cluster integral, and the spacing of two adjacent beads, respectively. Thus, q, M_L, and B may be regarded as the parameters characterizing the dimensional properties of the perturbed wormlike chain.

Experimental Section

Materials. Sodium hyaluronan (NaHA) was produced and purified in DENKA Co. Ltd. Japan from the culture medium of *Streptococcus equi*. Impurity was less than 0.02% as protein according to the Lowry method.[19] The original NaHA was degraded to four molecular weight fractions by thermal treatment. Each product was precipitated from 0.2 M aqueous NaCl solutions to the mixture of 95% acetone +5% water and dried in vacuo. Aqueous solutions of each fraction was treated by the mixed-bed ion exchanger and neutralized with 0.1 M NaOH. Dry NaHA samples were obtained by freeze-drying the solutions for 1 week. The intrinsic viscosities of these final products in 0.2 M NaCl solutions were 1180, 2480, 3000, and 5430 cm^3 g^{-1}, respectively, when measured by a Zimm−Crothers type rotating cylinder viscometer operating at a shear rate of 0.10 s^{-1}. A known weight of sample was dissolved in 0.2 M NaCl containing 0.02% NaN_3 as a biocide to prepare the desired sample solutions. Dissolution of NaHA samples were achieved by sufficiently gentle and occasional stirring over a few days at 4 °C in order to avoid possible degradation by shear.[20] The polymer concentration was determined by quantitative analysis of total organic carbon with a TOC-5000 (Shimadzu).

Conventional Light Scattering. We used a purpose-built light-scattering photometer and 240 channel digital correlator. Scattered light intensity measurements and the correlation function measurements using homodyne mode were carried out simultaneously. A vertically polarized He−Ne laser or an Ar ion laser operated at a wavelength λ_0 of 632.8 or 488.0 nm, respectively, was used as the incident beam. Vertically polarized scattered light was detected by a photomultiplier tube using the photon-counting method. Benzene was used as a standard for calibrating the scattering photometer.[21,22] A cylindrical cell of 10 mm outer diameter was placed in a thermostated silicon oil bath, the temperature of which was controlled with the constancy of 0.01 °C. Temperature was monitored by a calibrated platinum resistor. Optical purification of the sample was achieved by centrifugation (40000g) and filtration through cellulose acetate membrane filters (0.8 μm pore size).

Refractive Index Increments. The specific refractive index increment, $(\partial n/\partial c)_\mu$, of NaHA in 0.2 M NaCl at 25 °C was measured using a purpose-built Brice-type differential refractometer. The solution of NaHA in 0.2 M NaCl was dialyzed against 0.2 M aqueous NaCl at room temperature before the measurements. The

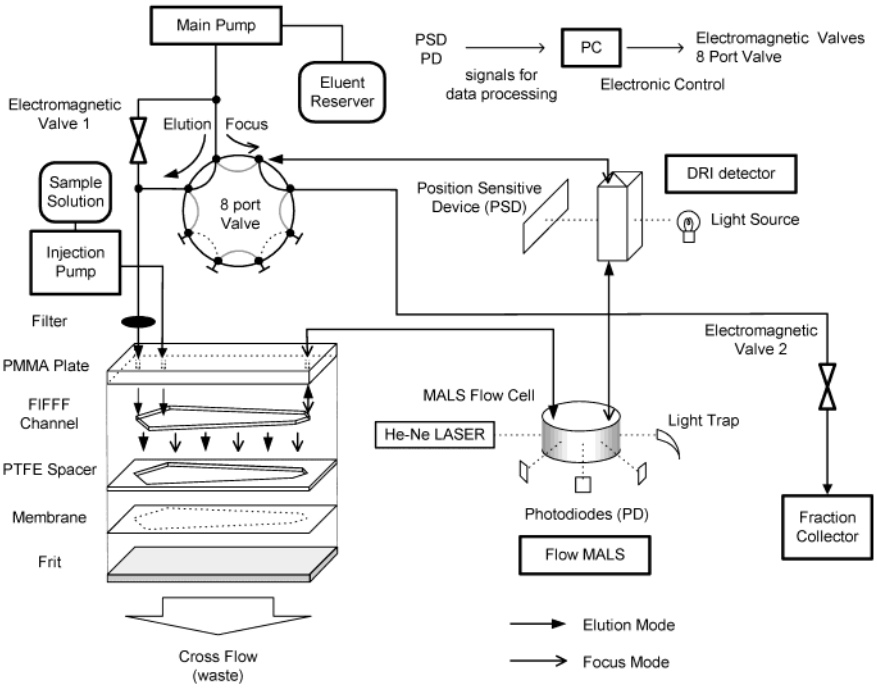

Figure 1. Schematic diagram of an asymmetrical FlFFF−MALS system.

values of 0.151 and 0.157 $cm^3\ g^{-1}$ were obtained for 633 and 488 nm of incident light, respectively.

Flow Field-Flow Fractionation−Multiangle Light Scattering (FlFFF−MALS). FlFFF experiments were carried out using an asymmetrical FlFFF fractionator 4.0 (ConSenxus GmbH) using a trapezoidal geometry. The channel was 28.6 cm long, and the trapezoid breadths were 2.12 and 0.47 cm, respectively. The area cut off at the inlet end was 2.25 cm^2, and the total area enclosed by the spacer was 36.09 cm^2. The nominal spacer thickness was 190 μm and the resulting channel volume 0.68 cm^3. The accumulation wall consisted of a Nadir UF-10C10 ultra filtration membrane of regenerated cellulose (Hoechst). A ConstaMetric 3200 pump was used to generate the flow in the channel. The injection of a sample was made with a Knauer pump (Microster K100). The eluent, which was filtered using a 0.2 μm membrane filter, was degassed before entering the channel by an ERC 3215α degasser. An in-line membrane filter with 0.1 μm pore size was installed between the main pump and the FlFFF channel. The performance of the channel was checked by color test with an aqueous solution of blue dextran. The focusing point was strictly positioned at 2 mm downstream from the sample inlet. The cross-flow rate and channel flow rate were 0.10 and 0.40 $cm^3\ min^{-1}$, respectively.

Multiangle static light-scattering measurements were made at 25.0 °C using a MALS detector of DAWN DSP (Wyatt Technology) with a vertically polarized He−Ne laser ($\lambda_0 = 633$ nm). The photometer, which was calibrated using pure toluene and aqueous solutions of low molecular weight dextran, was connected to the FlFFF channel and a differential refractive index detector OPTILAB DSP (Wyatt Technology), which was used to determine the concentration at each position of the peak. The setup of the asymmetrical FlFFF−MALS system is illustrated in Figure 1. The test solutions were filtered through 0.8 μm cellulose acetate membrane filters. Scattered light intensities at the scattering angle over 15−163° were measured; all available angles on the Wyatt MALS instrument were used.[23] The angular dependence of the scattering intensity was analyzed using Berry's square-root plot[24] to determine R_G and M at each position of the peak. 0.2 M aqueous NaCl solution was used as both the solvent and the eluent.

Table 1. Molecular Parameters Characterizing Sodium-Type Hyaluronan in 0.2 M NaCl at 25 °C Obtained via Conventional Light Scattering

sample code	$10^{-6} M_w$	$10^3 A_2$, $cm^3\ mol\ g^{-2}$	R_{Gz}, nm	$\mu_2/\bar{\Gamma}^2$
NH-1	0.667	1.95	96.0	0.14
NH-2	1.57	1.44	148	0.14
NH-3	2.15	1.43	180	0.13
NH-4	4.23	1.34	240	0.10

Results and Discussion

Conventional Light Scattering. The numerical data characterizing the solution properties of polydisperse NaHA in 0.2 M aqueous NaCl solution at 25.0 °C are tabulated in Table 1. The normalized variances, $\mu_2/\bar{\Gamma}^2$, determined from the correlation function measurements are also listed. The magnitudes of $0.1 \leq \mu_2/\bar{\Gamma}^2 \leq 0.14$ mean that our NaHA samples are relatively polydisperse, and the polydispersity is almost the same as the NaHA samples studied previously.[4]

In Figure 2, M_w dependence of R_{Gz} obtained from SLS measurements is shown. In this figure, the previously reported results[4] of R_{Gz} for NaHA in 0.2 M NaCl are plotted together with the present results. It is shown that both sets of data points coincide well with each other and the exponent ν of the linear fit for R_{Gz} is estimated as 0.58, whereas those from this study yield about 0.50 (dotted line).

According to Norisuye et al.,[9,17] NaHA in 0.2 M NaCl is a stiff wormlike chain, and the wormlike chain parameters are $q = 4.2$ nm, $M_L = 405\ nm^{-1}$, and $B = 4.0$ nm. It is notable that all the data points of R_{Gz} for polydisperse NaHA deviate clearly from the predicted curve of R_G using eqs 1 and 3 with wormlike chain parameters described above (long dashed line). This deviation should result from the substantial molecular weight distribution.

To examine the effect of molecular weight distribution on the magnitude of R_G, the z-average radius of gyration for

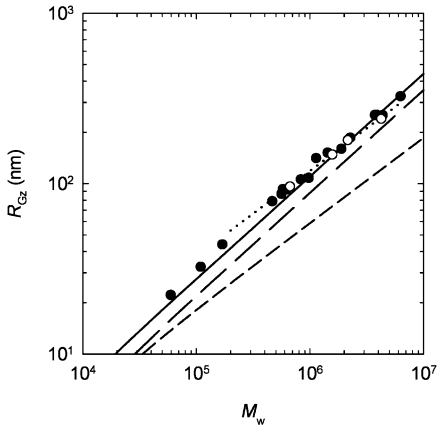

Figure 2. Comparison between the experimental and theoretical radii of gyration. The open and closed circles represent the *z*-average radii of gyration for present and previous (ref 4) results, respectively. The solid line represents the theoretical values calculated for polydisperse wormlike chain from eqs 1 and 3 with eq 6 for $q = 4.2$ nm, $M_L = 405$ nm^{-1}, $B = 4.0$ nm, and $M_w/M_n = 2.11$. The short dashed and the long dashed lines represent the unperturbed monodisperse and perturbed monodisperse wormlike chains, respectively. The dotted line is a linear fit of the present data.

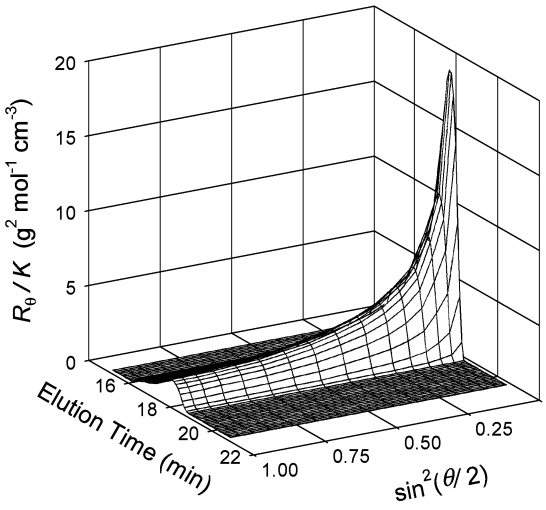

Figure 3. FlFFF−MALS 3D-chromatogram for polydisperse NaHA sample NH-4 in 0.2 M NaCl at 25 °C. *K* and R_θ are the optical constant and reduced excess scattering intensity, respectively. The sample concentration was 0.500 mg cm^{-3}. A 0.02 cm^{-3} injection loop was used.

polydisperse NaHA was analyzed by the Schulz−Zimm and log-normal distribution functions. In the Schulz−Zimm's framework, the weight fraction of the chain with a contour length L is given by[25]

$$w^{SZ} = \frac{(m+1)^{m+1}}{\Gamma(m+1)} \frac{L^m}{L_w^{m+1}} \exp\left[-\frac{(m+1)L}{L_w}\right] \qquad (5)$$

where m is the distribution parameter and $\Gamma(x)$ is the Gamma function. L_w is the weight-averaged contour length corresponding to M_w. If we assume $R_G = K_G M^\nu$, the ratio of R_{Gz} to that for a monodisperse sample having the same molecular weight, f^{SZ}, is

$$f^{SZ} = \frac{R_{Gz}}{R_G} \simeq \left[\frac{\Gamma(m+2+2\nu)}{(m+1)^{2\nu+1}\Gamma(m+1)}\right]^{1/2} \qquad (6)$$

On the other hand, the weight fraction of the chain for the log-normal type is written as

$$w^{LN} = \frac{1}{L[2\pi \ln(L_w/L_n)]^{1/2}} \exp\left[-\frac{1}{2\ln(L_w/L_n)}\left(\ln\frac{L}{L_w^{1/2}L_n^{1/2}}\right)^2\right] \qquad (7)$$

and the ratio f^{LN} is

$$f^{LN} = \frac{R_{Gz}}{R_G} \cong \left(\frac{m+1}{m}\right)^{\nu(2\nu+1)/2} \qquad (8)$$

In these equations, polydispersity indices are written as $M_w/M_n = 1 + 1/m$ or $M_z/M_w = (m+2)/(m+1)$. In Figure 2, the theoretical R_{Gz} of Shulz−Zimm polydisperse wormlike chain calculated for $q = 4.2$ nm, $M_L = 405$ nm^{-1}, $B = 4.0$ nm, and $f^{SZ} = 1.30$ ($M_w/M_n = 2.11$ and $M_z/M_w = 1.53$) is compared with the experimental results. The exponent value, ν, is adopted as 0.58. Relatively good agreement is observed between the theoretical curve and empirical data, indicating that the Shultz−Zimm distribution function with $M_w/M_n =$ 2.11 is a good approximation for our polydisperse NaHA. However, if we assume that the molecular weight distribution function of our NaHA is described by the log-normal-type with $f^{LN} = 1.30$, this distribution function yields $M_w/M_n = 1.53$ and $M_z/M_w = 1.34$.

As we have seen above, the polydispersity effect on R_G strongly depends not only on the degree of polydispersity but also on the shape of the molecular weight distribution. The reason that a value of 0.50 was obtained from this work for ν, which corresponds to the value for a Θ chain, is partly because the shapes of the distribution for each sample and/or the degree of polydispersity were different from each other. Thus, determination of the molecular weight distribution is essential for wormlike chain analysis of polydisperse samples. Determination of molecular weight distribution for stiff or rodlike polymers is, however, quite difficult even from SEC−MALS, due to the restrictions such as chain dimension and shear rate effects. The dynamic light-scattering−CONTIN[26] method is also not necessarily suitable for such analysis, because the contribution of intramolecular motions to the correlation function becomes enhanced for very large molecules.

FlFFF—MALS. In Figure 3, the three-dimensional FlFFF-chromatogram for the polydisperse NaHA sample NH-4 detected by MALS is depicted. Here, K is the optical constant and R_θ is the reduced excess scattering intensity at scattering angle θ. As shown in this figure, angular dependences of scattered light at each elution time are clearly observed. Furthermore, it is worth noting that the analysis time for NH-4 was very short and was less than 20 min.

Figure 4 shows the values of $(Kc/R_\theta)^{1/2}$ for the three typical fractions of NaHA in 0.2 M aqueous NaCl solution plotted against $\sin^2(\theta/2)$, where c is the polymer mass concentration. Although centrifugation was not performed to remove the unnecessary dusts in the test solutions, good precision was observed for all the available angles on the well-calibrated Wyatt MALS instrument; as for the conventional static light-

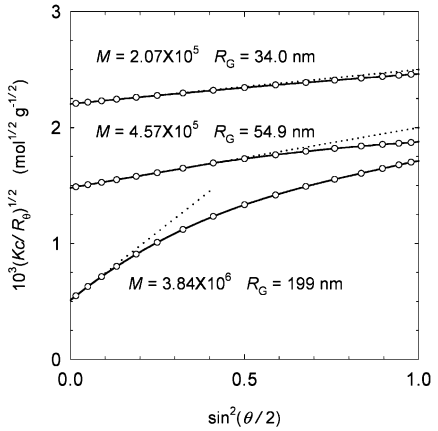

Figure 4. Angular dependences of $(Kc/R_\theta)^{1/2}$ for fractionated NaHA by asymmetrical FlFFF.

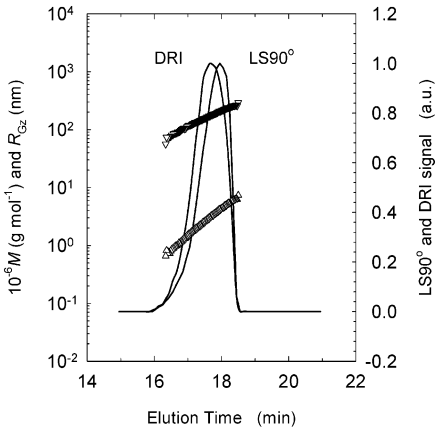

Figure 5. Molecular weights (triangle up) and radii of gyration (triangle down) vs elution time for NH-4. Lines represent the DRI and light scattering at 90° signals. The measurement was carried out in 0.2 M NaCl at 25 °C. The cross-flow rate was 0.1 cm^3 min^{-1}, and channel flow rate was 0.4 cm^3 min^{-1}. The sample concentration was 0.500 mg cm^{-3}. A 0.02 cm^{-3} injection loop was used.

scattering measurements, centrifugation was always necessary to obtain good precision at lower scattering angles. The dusts might be accumulated on the ultra filtration membrane, and signal-to-noise ratio kept high value (see Figure 3). The dotted lines in Figure 4 represent the initial slopes to the curves obtained for the experimental $(Kc/R_\theta)^{1/2}$ at infinite dilution by the least-squares fit. The curves fitting to the data points are more convex upward for higher molecular weight. In this work, to evaluate the accurate sets of M and R_G from the MALS profiles,[27] the effects of concentration on Kc/R_0 were compensated using a relation of $A_2 = 0.022M_w^{-0.19}$ (cm^3 mol g^{-2}), which was estimated from previous[4] and present results (applicable to $10^4 < M_w < 10^7$), although our values of A_2Mc at each position of the peaks was generally less than 0.01. From the final results of the intercepts with the ordinate and the initial slopes against the scattering angle, M and R_G at each position were calculated for all samples, respectively.

In Figure 5, M and R_G vs the elution time is displayed for the NH-4 sample together with the corresponding differential refractive index (DRI) and SLS at the scattering angle of 90° signals. The DRI and SLS 90° signals do not overlap due to the molecular weight distribution of the sample, because the DRI detector is sensitive only to polymer mass,

Table 2. Comparison between the Results from Conventional Light Scattering and Those from FlFFF−MALS[a]

	$10^{-6}M_z$	$10^{-6}M_w$	$10^{-6}M_n$	M_z/M_w	M_w/M_n	R_{Gz}, nm
		Sample NH-1				
conventional		0.667		1.56		96.0
FlFFF-MALS	1.09	0.700	0.486	1.56	1.44	95.0
ratio		1.05		1.00		0.99
		Sample NH-2				
conventional		1.57		1.56		148
FlFFF-MALS	2.35	1.63	1.16	1.44	1.40	152
ratio		1.04		0.92		1.03
		Sample NH-3				
conventional		2.15		1.52		180
FlFFF-MALS	3.62	2.21	1.57	1.54	1.41	173
ratio		1.03		1.01		0.96
		Sample NH-4				
conventional		4.23		1.40		240
FlFFF-MALS	6.31	4.36	3.50	1.44	1.25	249
ratio		1.03		1.03		1.04

[a] Ratio is [FlFFF−MALS]/[conventional].

whereas the SLS signal is sensitive to both the polymer mass and chain dimension. The two peaks will overlap for a monodisperse sample or for a homogeneous mixture of many different sizes. The latter will for example be obtained if there is no size separation at all. It is clearly seen that there are increases in M and R_G as a function of the elution time. The noises in the M and R_G curves in the large and small elution volume regions are due to the low concentration of polymer, which makes the calculated molecular weight unreliable in this area, although it will not have any significant influence on M_w and R_{Gz} calculated over the entire peak.

The data of M_z, M_w, M_n, and R_{Gz} calculated are summarized and compared with the results from conventional SLS in Table 2. In the fourth and fifth columns, M_z/M_w and M_w/M_n are also listed. The values of M_z/M_w in the rows for conventional light scattering were estimated using a relation of $M_z/M_w \sim 1 + 4(\mu_2/\bar{\Gamma}^2)$.[28] The agreements are fairly good for M_w and R_{Gz}, and the deviation is at most only 5%. In fact, the recovery rates were generally above 95% for all of the samples we tested, indicating that the polymer did not permeated through the accumulation wall, which has a pore size of 2.4 nm. Adsorption and shear degradation were minimal in the FlFFF channel.[29]

In Figure 6, the theoretical curves of R_G for NaHA in 0.2 M NaCl calculated from Yamakawa−Stockmayer−Shimada theory for perturbed wormlike chain (eqs 1 and 3) are compared with the experimental R_G obtained via FlFFF−MALS. Here, the persistence length q and the molecular weight per unit contour length M_L are adopted as 4.2 and 405 nm^{-1}, respectively. The experimental R_G shows a good agreement with the predictions of the perturbed wormlike chain theory in the molecular weight range from 10^5 to 10^7 if the excluded volume strength B is assumed to be 4.0 nm. Dimensional behavior of sodium hyaluronan in 0.2 M NaCl is well expressed by the Yamakawa−Stockmayer−Shimada theory with parameters of $q = 4.2$ nm, $M_L = 405$ nm^{-1}, and $B = 4.0$ nm up to $M_w = 10^7$.

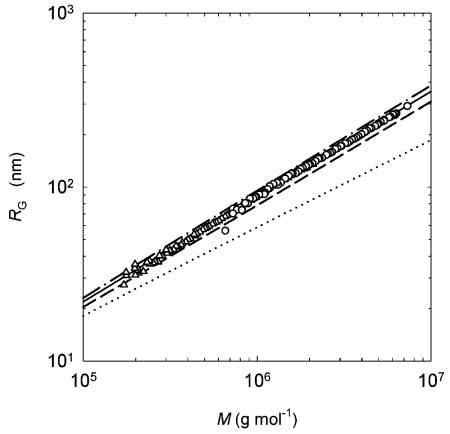

Figure 6. Comparison between experimental and theoretical radii of gyration. The triangles and circles represent the radii of gyration for NH-1 and NH-4, respectively. The solid line represents the theoretical values calculated from eq 3 with eq 1 for $q = 4.2$ nm, $M_L = 405$ nm^{-1}, and $B = 4.0$ nm, and dashed and dot−dashed lines represent the calculated ones for $B = 2.0$ and 6.0 nm, respectively. The dotted line refers to the unperturbed wormlike chain.

Conclusion

This study clearly demonstrated that it is possible to use FlFFF−MALS to obtain reliable results regarding not only averaged molecular weight and radius of gyration, but accurate relationship of M and R_G even for weakly stiff chains. It seems that SEC−MALS can be used for the wormlike chain analysis, however, this method has definitive disadvantages such as adsorption, shear degradation, and size exclusion limit. As for hyaluronan, one of the weakly stiff chains, no size separation or shear degradation often occurs in a SEC column. FlFFF−MALS may overcome all the probable problems described above. It should be noted that FlFFF−MALS provides a relationship between M and R_G in a shorter time period in comparison to SEC−MALS, and is applicable to size separation of weakly stiff chains having very high molecular weight. This is a great advantage for the characterization of polymers and to the study of solution properties such as wormlike chain analysis. The only one shortcoming of FlFFF−MALS is that there is a difficulty of channel settings (determination of the flow condition) to get reliable results. The size separation quality of a FlFFF channel strongly depends on ideality of the flow lines, or axial and cross-flow streamlines. Further studies will focus on defining both the flow channel geometry and the adequate flow condition in the channel.

Acknowledgment. R.T. and K.N. thank Unilever for the financial support.

References and Notes

(1) Kratky, O.; Porod, G. *Recl. Trav. Chim. Pays-Bas* **1949**, *68*, 1106−1222.
(2) Yamakawa, H. In *Helical Wormlike Chains in Polymer Solutions*; Springer-Verlag: Berlin, 1997.
(3) For example, Fujita, H. *Polymer Solutions*; Elsevier: Amsterdam, 1990.
(4) Takahashi, R.; Kubota, K.; Kawada, M.; Okamoto, A. *Biopolymers* **1999**, *50*, 87−98.
(5) Takahashi, R.; Akutu, M.; Kubota, K.; Nakamura, K. *Prog. Colloid Polym. Sci.* **1999**, *114*, 1−7.
(6) Kulicke, W. -M.; Böse, N. *Colloid Polym. Sci.* **1984**, *262*, 197−202.
(7) Wahlund, K.-G. In *Field-Flow Fractionation Handbook*; Schimpf, M., Caldwell, K., Giddings, J. C., Eds.; Wiley-Interscience: New York, 2000; Chapter 18.
(8) Wittgren, B.; Wahlund, K.-G. *J. Chromatogr. A* **1997**, *791*, 135−149.
(9) Hayashi, K.; Tsutsumi, K.; Nakajima, F.; Norisuye, T.; Teramoto, A. *Macromolecules* **1995**, *28*, 3824−3830.
(10) Yamakawa, H.; Fujii, M. *Macromolecules* **1974**, *7*, 128−135.
(11) Yamakawa, H.; Yoshizaki, T. *Macromolecules* **1980**, *13*, 633−643.
(12) Yamakawa, H.; Stockmayer, W. H. *J. Chem. Phys.* **1972**, *57*, 2843−2854.
(13) Yamakawa, H.; Shimada, J. *J. Chem. Phys.* **1985**, *83*, 2607−2611.
(14) Shimada, J.; Yamakawa, H. *J. Chem. Phys.* **1986**, *85*, 591−600.
(15) Barrett, A. J. *Macromolecules* **1984**, *17*, 1566−1572.
(16) Domb, C.; Barrett, A. J. *Polymer* **1976**, *17*, 179−184.
(17) Tsutsumi, K.; Norisuye, T. *Polym. J.* **1998**, *30*, 345−349.
(18) Benoit, H.; Doty, P. *J. Phys. Chem.* **1953**, *53*, 958−963.
(19) Lowry, O. H.; Rosebrough, N. J.; Farr, A. L.; Randall, R. J. *J. Biol. Chem.* **1951**, *193*, 265−275.
(20) Miyazaki, T.; Yomota, C.; Okada, S. *J. Appl. Polym. Sci.* **1998**, *67*, 2199−2206.
(21) Pike, E. R.; Pomeroy, W. R. M.; Vaugham, J. M. *J. Chem. Phys.* **1975**, *62*, 3188−3192.
(22) Chu, B.; Onclin, M.; Ford, J. R. *J. Phys. Chem.* **1984**, *88*, 6566−6575.
(23) The MALS K5 flow cell was disassembled and cleaned completely just before calibrating the DAWN instrument. This procedure is essential to get good precision at the lowest scattering angle.
(24) Berry, G. C. *J. Chem. Phys.* **1967**, *46*, 1338−1352.
(25) Zimm, B. H. *J. Chem. Phys.* **1978**, *16*, 1099−1116.
(26) Provencher, S. W. *Comput. Phys. Commun.* **1982**, *27*, 213−228.
(27) More precisely, M and R_G in Figures 4, 5, and 6 should be weight-averaged and z-averaged quantities, respectively, because the MALS−DRI detection measures the averages in slice of the elution profile. This means each position in the fractogram may contain a more or less narrow distribution of sizes depending on the quality of the fractogram. In this paper, however, M and R_G are adopted to avoid confusion with M_w and R_{Gz} obtained from conventional static light-scattering measurements.
(28) Pusey, P. N. In *Photon Correlation and Light Beating Spectroscopy*; Cummins, H. Z., Pike, E. R., Eds.; Plenum Press: New York, 1974.
(29) Wahlund, K.-G.; Giddings, J. C. *Anal. Chem.* **1987**, *59*, 1332−1339.

BM025706V